

Nucleate pool boiling heat transfer and critical heat flux of FK-649 on an inverter power module

Ilya T'Jollyn^{1,2}, Jasper Nonneman^{1,2}, Wim Beyne¹ and Michel De Paepe^{1,2}

¹ Department of Electromechanical, Systems and Metal Engineering, Faculty of Engineering and Architecture, Ghent University, Sint-Pietersnieuwstraat 41, Ghent, Belgium

² FlandersMake@UGent – Core lab EEDT-MP, Leuven, Belgium

Ilya.TJollyn@UGent.be

ORCID

Ilya T'Jollyn: 0000-0003-3151-260X

Jasper Nonneman: 0000-0001-6196-3757

Wim Beyne: 0000-0002-7450-9382

Michel De Paepe: 0000-0003-0233-0719

Abstract. Measurements on heat transfer and critical heat flux of pool boiling cooling of the baseplate of an inverter power module are performed. A refrigerant with low global warming potential, FK-649, is used as coolant. Tests are done for heat fluxes up to 146 kW/m², with refrigerant saturation temperatures of 36 °C, 41 °C and 46 °C and with refrigerant liquid heights of 1 cm, 6 cm and 17 cm. Both heat transfer rates and critical heat flux increase with increasing saturation temperature. In the range tested, the liquid height had no effect on both the boiling curve and the critical heat flux. The measured boiling curve can be divided in three regions: two regions with a lower slope at heat fluxes just above onset of nucleate boiling and just below the critical heat flux and a region with a higher slope at intermediate heat fluxes. The measured critical heat flux for FK-649 is predicted by the Lienhard-Dhir correlation within 10%. The highest critical heat flux measured is 146 kW/m², which is lower than the heat fluxes in the most compact power modules. This indicates that methods to increase the critical heat flux are needed for enabling two-phase power module cooling with FK-649.

1. Introduction

Electrification in the transport sector is globally on the rise. To increase the efficiency and range of electric vehicles, drivetrains need to become ever more power dense [1]. By increasing the power rating of components while reducing their volume, cooling requirements become more stringent to avoid overheating and failure. The power module of the inverter is one of the critical components in the drivetrain, with heat fluxes exceeding 300 kW/m². The state-of-the-art cooling method for the power modules is forced liquid cooling, usually with a water-glycol mixture. In this study, cooling with boiling refrigerants is experimentally investigated. This method features high heat transfer coefficients, low pumping power and can possibly reduce the size of the heat sink [2].

For designing two-phase cooling systems, the component temperature should be predicted from the component heat flux and coolant saturation temperature. For pool boiling heat transfer, the heat flux

(component heat dissipation per area) is typically correlated to the surface superheat temperature, which is the difference of the surface (component) temperature and the saturation (coolant) temperature. This relation is typically referred to as the boiling curve and is thus crucial to be able to predict boiling heat transfer. Many correlations have been proposed to predict the boiling curve, however large deviations with measurements, up to 40%, are commonplace [3]. It therefore remains crucial to experimentally determine the boiling curves for new refrigerants.

A plausible reason for the high deviations of the correlations, can be that the entire nucleate boiling regime is described by one power-law equation. However, different behaviours of the boiling curve can be perceived at low heat fluxes (close to the onset of nucleate boiling) and at high heat fluxes (close to the critical heat flux). This is clear in the experimental results of El-Genk and Bostanci [4] on pool boiling heat transfer of refrigerant HFE-7100, where a high slope of the boiling curve is measured in the moderate heat flux region and lower slopes in the low and high heat flux region. They proposed a new correlation which considers the three different regions. This correlation however is only valid for refrigerant HFE-7100 and it is not yet clear if this behaviour of the boiling curve is applicable to other refrigerants.

Although two-phase cooling entails high heat transfer rates, a major risk is associated to it as well. When the heat flux increases to a certain limiting value, a vapour film is formed over the entire cooled surface [5]. This vapour film acts as an insulator, drastically reducing the heat transfer rates and thus causing overheating of the power module. Next to the boiling curve, it is therefore also of utmost importance to know this maximal heat flux, commonly called the critical heat flux (CHF). Liang and Mudawar [6] made a thorough review of the available correlations for CHF in scientific literature. For horizontal, upward facing configurations, the best performing correlations are those of Lienhard and Dhir [7] (which adds a correction on the leading constant of the correlation of Zuber [5]) and of Mudawar et al. [8]. The correlation of Lienhard and Dhir is given by:

$$CHF = 0.149 \rho_v^{1/2} h_{lv} [\sigma g (\rho_l - \rho_v)]^{1/4} \quad (1)$$

In this equation, ρ_v is the vapour density, h_{lv} is the latent heat of vaporisation, σ is surface tension, g is the gravitational acceleration and ρ_l is the liquid density. If there is no subcooling and the pressure is substantially lower than the critical pressure, the correlation of Mudawar et al. reduces to equation 1 with the leading constant changed from 0.149 to 0.151.

There are a limited number of studies available in scientific literature on pool boiling cooling of power electronic modules. The National Renewable Energy Laboratory (NREL) tested direct baseplate pool boiling cooling of a power module using refrigerants HFE-7100 and R134a [9]. Heat transfer coefficients up to 13000 W/m²K for the refrigerant HFE-7100 and 50000 W/m²K for the refrigerant R134a were measured for boiling on a plain copper baseplate. Higher values were achieved by using engineered microporous and nanostructured surfaces. The critical heat flux values were 210 kW/m² for HFE-7100 and 600 kW/m² for R134a. Barnes and Tuma [10] tested pool boiling cooling of an insulated-gate bipolar transistor (IGBT) module, where both the IGBT and baseplate were in direct contact with the fluid. The tested fluid was refrigerant HFE-7000. The module was tested with a standard copper baseplate and with a microporous coated baseplate. Heat transfer coefficients and critical heat fluxes were reported based on the IGBT die area and not on the baseplate area, so these cannot be directly compared to those cited above. Barnes and Tuma [10] concluded that the total thermal resistance of a directly cooled IGBT module could be 50% to 70% lower than that of a traditional liquid cooled module.

Although pool boiling is thoroughly studied for electronics cooling, most studies feature refrigerants such as FC-72 and R-113, which have a high global warming potential (GWP). Recently, low-GWP alternatives have been introduced, such as refrigerants HFE-7000, HFE-7100 and FK-649, of which the later will be the fluid investigated in this study. Table 1 gives an overview of the pool boiling studies conducted with FK-649. The overview in the table is limited to standard flat surfaces, other geometries (wires, tubes) and engineered surfaces are not included, as these are of less interest for this work. Forrest et al. [11] show that pool boiling heat transfer of FK-649 is similar to that of FC-72 with the advantage of a much lower GWP. In a different study, Forrest et al. [12] report on measurements of FK-649 boiling on an aluminium disc. Gess et al. [13] investigated two-phase immersion cooling on bare dies for data

centres. Kaniowski et al. [14] tested pool boiling on a copper surface for microelectronic chip cooling. Electric motor winding cooling was envisaged and tested by Bartle et al. [15]. Ghaffari et al. [16] performed experiments on pool boiling of FK-649 and HFE-7100 for microprocessor cooling. Both fluids featured similar heat transfer rates, but the CHF was about 20% higher for HFE-7100. Cao et al. [17] experimentally determined the boiling curve of FK-649 on a smooth copper surface. Of these studies, only one study (Forrest et al. [12]) experimentally determined the influence of the saturation temperature and pressure. Saturation pressures below atmospheric have not yet been tested.

Table 1 List of studies on pool boiling of FK-649.

Author(s)	T_{sat} [°C]	\dot{q} [kW/m ²]
Forrest et al. [11, 12]	49 – 96	5 – 215
Gess et al. [13]	49	5 – 120
Kaniowski et al. [14]	49	5 – 70
Bartle et al. [15]	49	10 – 75
Ghaffari et al. [16]	49	40 – 195
Cao et al. [17]	49	5 - 173

The goal of this paper is to experimentally investigate the heat transfer and critical heat flux of pool boiling cooling of the baseplate of an inverter power module. The effect of saturation temperature and pressure below atmospheric pressure is analysed. Furthermore, the experimental results for the critical heat flux are compared to the predictions of the most used correlations.

2. Experimental setup

The inverter power module used in this research is an Infineon HybridPACK type FS400R07A1E3, shown in figure Fig. 1. It consists of a six-pack with IGBTs and diodes. This is a typical module used in the inverter of a drivetrain, with a rated voltage and DC current of respectively 650 V and 400 A.

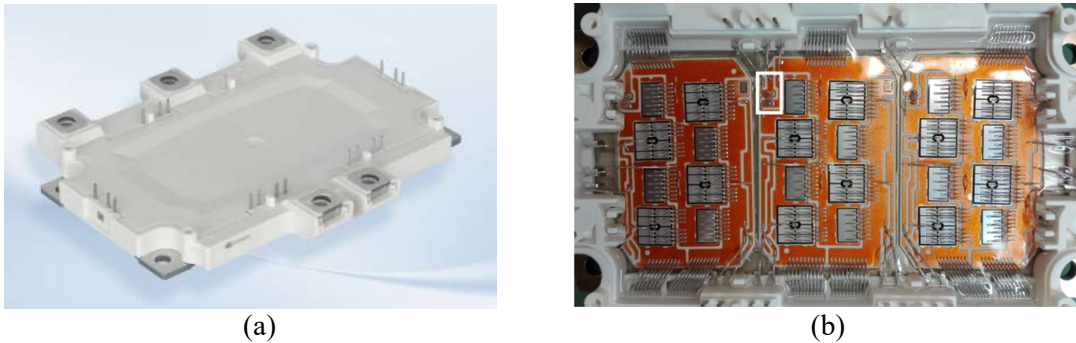


Fig. 1 Infineon power module (a) and its interior (b)

In a previous study, a three-phase current waveform was applied to the module to provide losses in the IGBTs and diodes [18]. This approach was accompanied by some drawbacks. As the losses in the power module are two orders of magnitude smaller than the electrical power, a circuit containing a second power module and inductors was added. This allowed for the three-phase power to be circulated between the components and thus only the electrical losses needed to be supplied by a power source. However, due to the current limitation of the inductors of 50 A, the power dissipation in the module was limited. This power dissipation in the module could only be measured indirectly through the heat balance, as the high switching frequency of the waveform required a too high sample frequency for accurately determining the power from voltage and current measurements.

To solve the previously mentioned issues, in this study power dissipation in the module is achieved by applying a DC current to the IGBTs. The gate voltage of the IGBTs is chosen such that it operates in

the active region. In this region, the current remains quasi constant while the voltage can be adjusted to vary the power losses in the module. With this method, heat dissipation rates up to 300 kW/m² can be achieved in the module. Furthermore, the electrical power can be accurately measured from the module DC voltage and current. In this configuration, all current will flow through the IGBTs and no current through the diodes. This is thus the worst case for the thermal load of the IGBTs.

The baseplate of the power module, which has an arithmetic mean surface roughness of 0.2 μm, is cooled by direct contact with a refrigerant. For this study, C₂F₅C(O)CF(CF₃)₂ or 1,1,1,2,2,4,5,5,5-nonafluoro-4-(trifluoromethyl)-pentan-3-one is chosen as coolant. This fluid is also commonly known by its trade name Novec 649 or by FK-649, as it is a fluoroketone (FK). It has a boiling point of 49 °C at atmospheric pressure, making it viable for immersion cooling of electronics. Its main advantages are the high dielectric strength, non-flammability, non-toxicity and a low global warming potential equal to 1.

The refrigerant is contained in a leak-tight stainless-steel reservoir with a height of 330 mm, length of 176 mm and width of 213 mm, shown in figure Fig. 2. The reservoir can be filled with a variable amount of refrigerant, leading to different liquid heights above the boiling surface. The power module is bolted to the bottom plate with a silicon gasket in between to avoid leakage of refrigerant between the plates. The bottom plate has a rectangular cut-out with dimensions 108 mm by 47 mm to form the boiling surface on the baseplate. The bottom plate is made of 8 mm thick polyoxymethylene (POM). This material was chosen to limit additional heat flows from the baseplate to the bottom plate, as it has a low thermal conductivity (0.35 W/mK) compared to metals. The reservoir is cooled by a spiral condenser at the top. This copper tube carries a water-glycol mixture which is pumped through it to provide cooling. To avoid heat losses from the reservoir to the environment, the reservoir is insulated with a 5 cm thick layer of polyurethane with a thermal conductivity of 0.025 W/mK (not shown on figure Fig. 2).

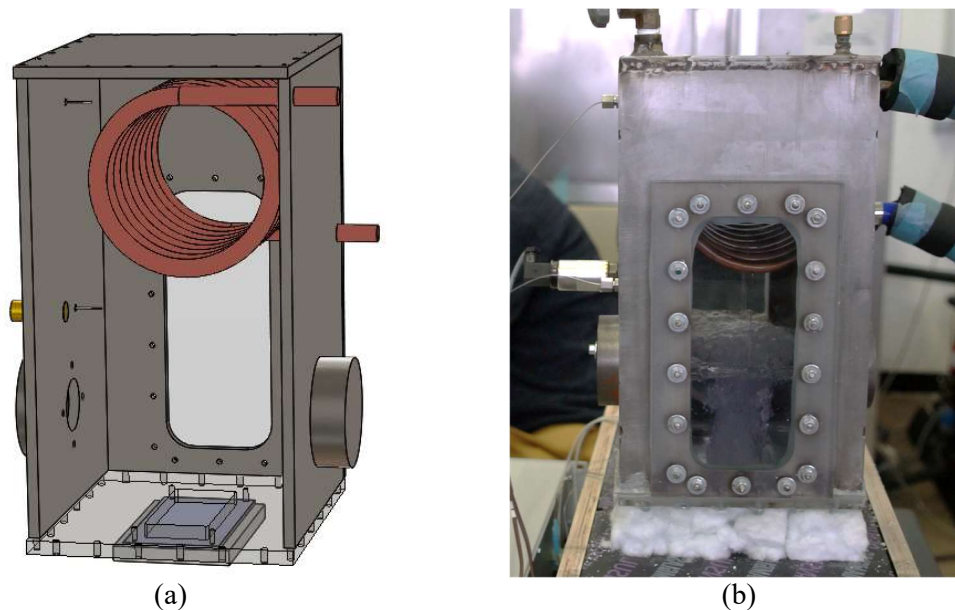


Fig. 2 Refrigerant reservoir: CAD drawing without front plate (a) and picture (b)

To analyse the cooling performance, the temperature difference between the baseplate and the refrigerant (or surface superheat temperature) and the heat flux must be measured.

The baseplate temperature is measured by three K-type mineral insulated thermocouples. These thermocouples are placed in between the baseplate and the silicon gasket, providing direct contact with the baseplate but not with the refrigerant. With this configuration, the baseplate temperature can be

measured without affecting the boiling phenomenon. The three thermocouples are equally spaced along the long side of the boiling surface.

The refrigerant temperature is measured at two locations by type T mineral insulated thermocouples. However, as significant thermal gradients are measured in the vapour phase, these measurements are not always a good indication of the refrigerant saturation temperature. The pressure in the reservoir is monitored by a pressure transducer. As there always exists a two-phase state within the reservoir, this pressure can be linked to the saturation temperature through the refrigerant saturation curve. To determine the surface superheat temperature, the thermocouple measurement is used when it is in direct contact with the liquid refrigerant. If it is not in direct contact, the saturation temperature derived from the pressure measurement is used.

The heat flux is determined from the voltage and current measurements. The voltage is measured directly at the module terminals to avoid inaccuracies due to voltage drops in the connecting cables. The current is measured by the DC source used to supply the power.

To analyse potential heat losses, the energy balance of the setup is determined. The energy going out of the reservoir with the water-glycol mixture, or net efflux, is determined using temperature measurements and a volumetric flow meter. The temperatures at inlet and outlet of the spiral condenser are measured by type T mineral insulated thermocouples. The volumetric flow rate is determined with an oval gear flow meter. The net efflux E_{net} is determined as:

$$E_{net} = \rho \dot{V} (h_o - h_i) \quad (2)$$

In this equation, ρ is the water-glycol mixture density, \dot{V} is the volumetric flow rate, h_o is the specific enthalpy of the water-glycol mixture leaving the condenser and h_i that of the incoming mixture. The density and enthalpies are determined based on the measured temperatures using the fluid-property library CoolProp [19].

An overview of all the sensors and their measurement uncertainties is given in table 2.

Table 2 Sensors and their measurement uncertainty.

Sensor	Uncertainty
Thermocouple	± 0.07 °C
Pressure transducer	± 720 Pa
Current	± 0.24 A
Voltage	± 50 μ V $\pm 0.003\%$
Flow rate	$\pm 1.5\%$

3. Results and analysis

3.1. Energy balance

The heat losses of the setup are analysed using the experimentally measured energy balance. The net efflux of energy is shown as a function of the dissipated power in the module in figure Fig. 3. For most measurement points, the net efflux is slightly lower than the dissipated power, indicating some heat losses.

The relative deviation of the energy balance is shown in figure Fig. 4. The relative deviation decreases significantly with heat flux, which is the result of the increasing heat transfer coefficient of nucleate boiling heat transfer with heat flux. From a heat flux of 65 kW/m², the energy balance closes within 5% and from 100 kW/m² it remains within 3%. This indicates that for the heat fluxes higher than 65 kW/m², the actual surface heat flux will be within 5% of the heat flux determined from the electrical power dissipation.

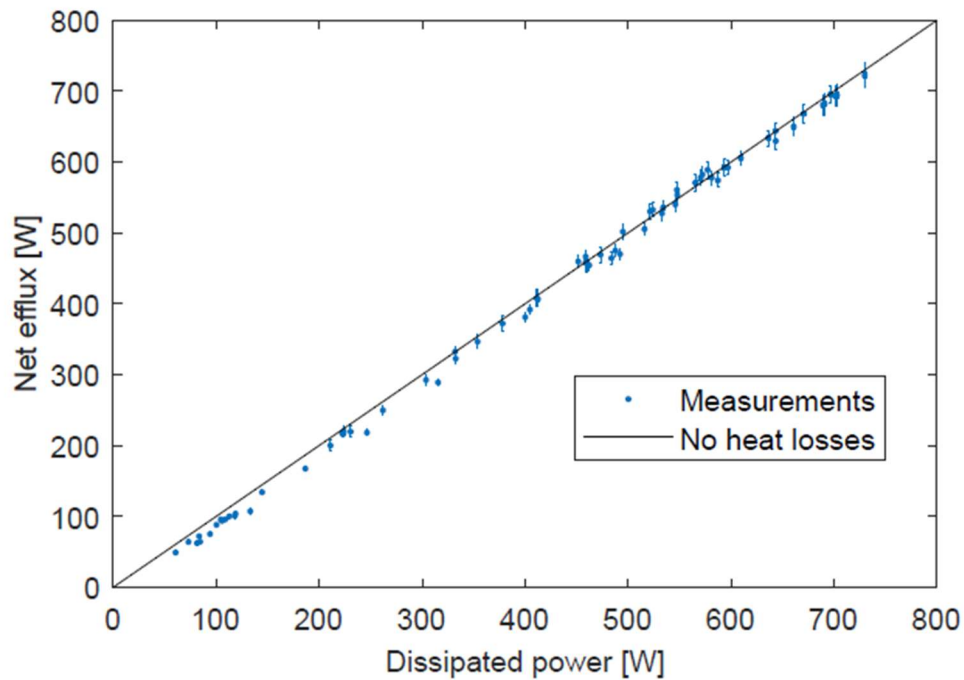


Fig. 3 Net efflux as a function of electrical power

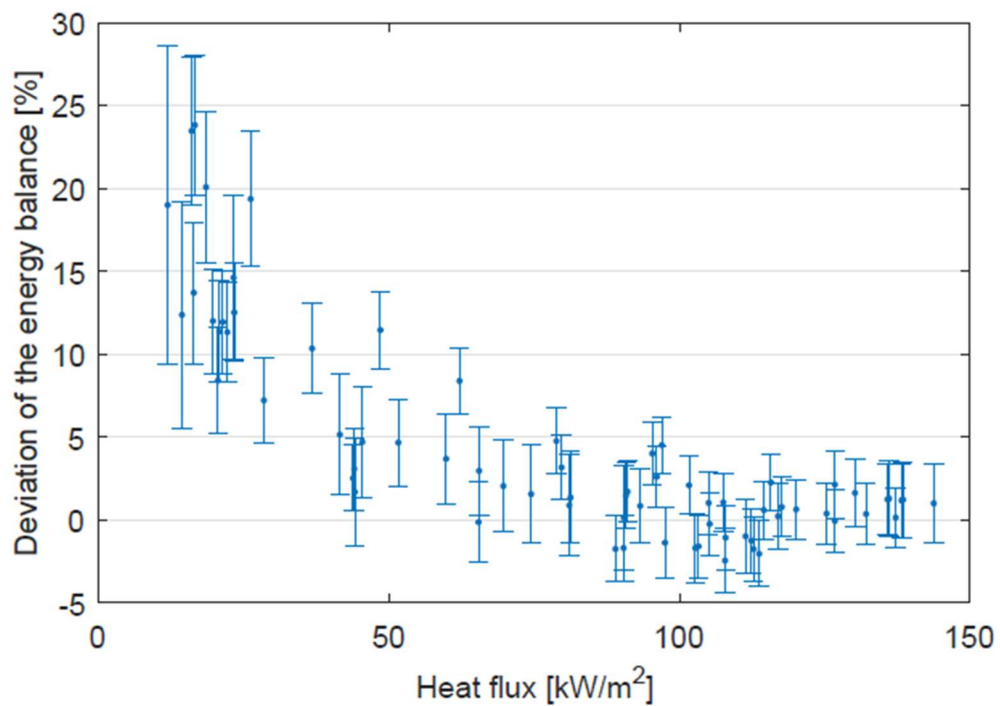


Fig. 4 Relative deviation of the energy balance as a function of heat flux

3.2. Boiling curve

Figure Fig. 5 shows the boiling curve for a saturation temperature of 36 °C and a liquid height of 1 cm. All measurement points are in the nucleate boiling region (except for the cross marker which is at the critical heat flux), no points of the natural convection region are included. The measurements were spread over several days, with several points repeated at different instances to check repeatability of the

measurements. Both horizontal error bars for the temperature difference and vertical error bars for the heat flux are shown in figure Fig. 5. For the clarity of the figures, the error bars are not shown on most of the following figures.

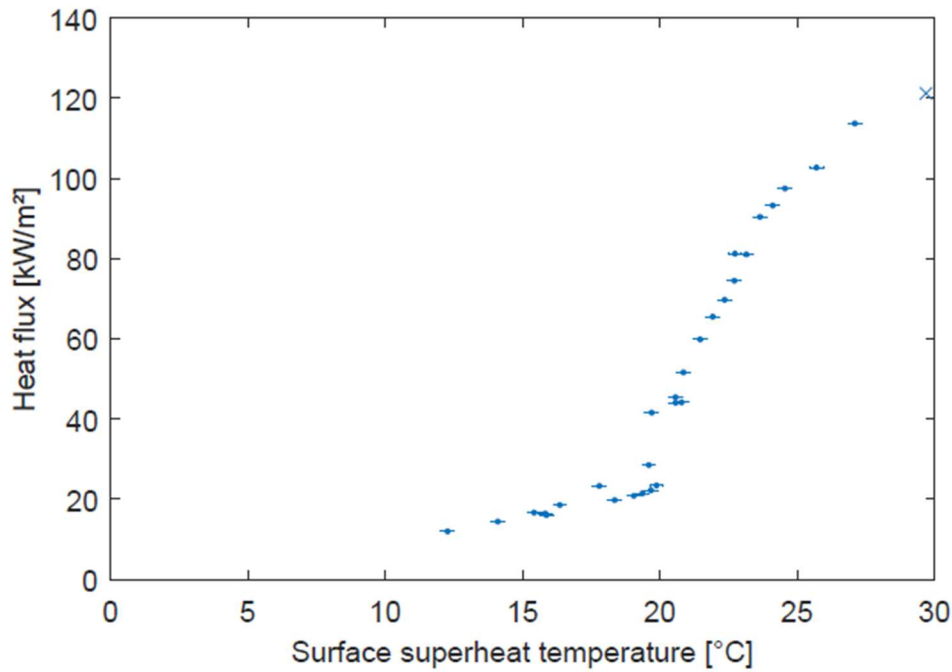


Fig. 5 Boiling curve for a saturation temperature of 36 °C and a liquid height of 1 cm, the cross marker indicates critical heat flux

In the boiling curve, three different zones with different slopes can be clearly distinguished. The initial zone with lower slope lasts up to heat fluxes around 20 kW/m². The second zone, where the slope of the boiling curve is significantly higher, ranges from 20 kW/m² to about 90 kW/m². For even higher heat fluxes, the slope of the boiling curve starts to decrease again until the maximum heat flux is reached. This behaviour is consistent with the observations of El-Genk and Bostanci [4].

Three different liquid heights are tested: 1 cm, 6 cm and 17 cm. All measurement points for a saturation temperature of 36 °C are shown in figure Fig. 6. Most measurements were done at the lowest liquid level, while the full boiling curve is also measured for the highest liquid level. For the medium liquid level, only two points were taken for reference. All these points fall onto the same boiling curve. For the liquid height range between 1 cm and 17 cm, it is concluded that there is a negligible influence of the liquid height on the boiling curve. In the following section, the measurement points for different liquid heights are shown together, as also for other saturation temperatures, the liquid height does not affect the boiling curve.

The boiling curve was measured for saturation temperatures equal to 36 °C, 41 °C and 46 °C. These boiling curves are shown in figure Fig. 7. For saturation temperatures of 41 °C and 46 °C, the partial nucleate boiling region was not measured as this is of less importance for electronics cooling and as the uncertainty on the energy balance is relatively high because of the low heat flux. The heat transfer rates increase with increasing saturation temperature. This behaviour corresponds with the measurements of Forrest et al. [12], where higher saturation temperatures were tested which resulted in lower surface superheat temperatures for identical heat fluxes. As a results, the highest heat transfer coefficient measured in this study was at a saturation temperature of 46 °C and is equal to 5000 W/m²K.

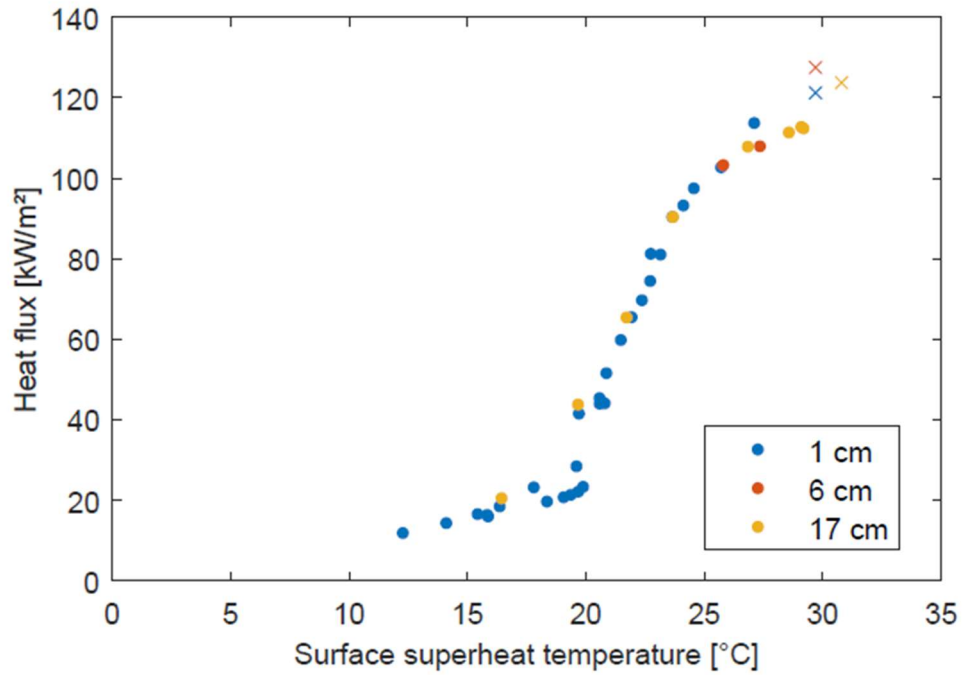


Fig. 6 Boiling curves for a saturation temperature of 36 °C and varying liquid height

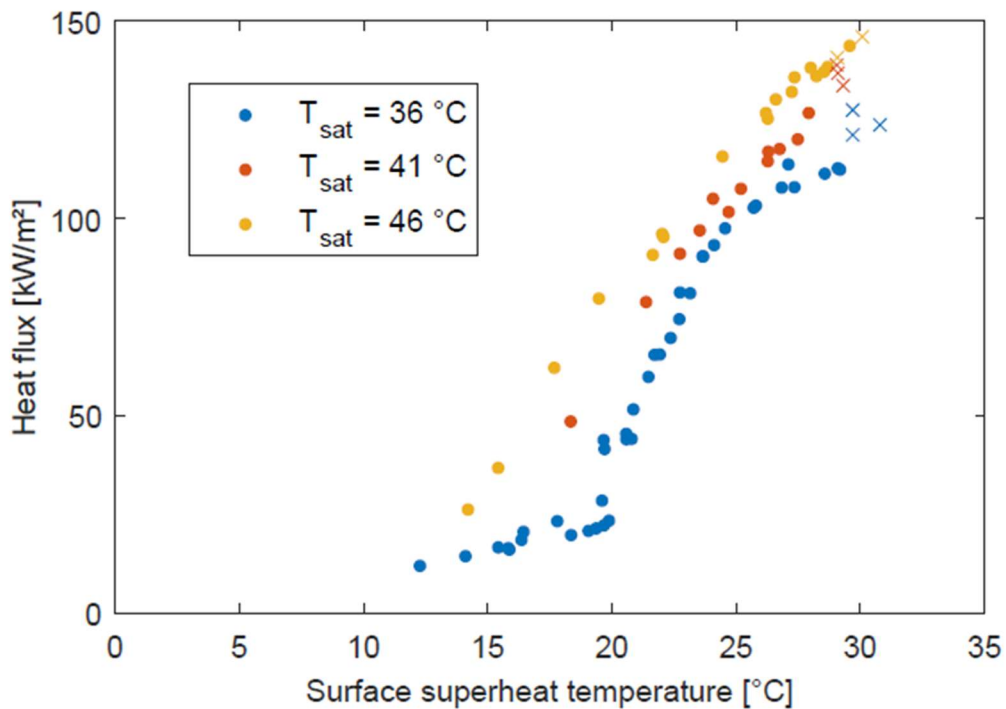


Fig. 7 Boiling curves for varying saturation temperatures

3.3. Critical heat flux

The critical heat flux as a function of the refrigerant saturation temperature is shown in figure Fig. 8. In the range investigated in this study (34 °C to 46 °C), CHF increases with saturation temperature. The measured CHF ranges from 121 kW/m² to 146 kW/m². Figure Fig. 8 also shows the influence of the liquid height on CHF. For similar saturation temperatures, the measured CHF lies within 3% for the

different liquid heights (1 cm, 6 cm and 17 cm). The minor differences show no clear correlation with liquid height and are attributed to the uncertainties in determining the CHF. In the range of liquid heights tested in this study (1 cm to 17 cm), the influence of the liquid height on the CHF is thus negligible.

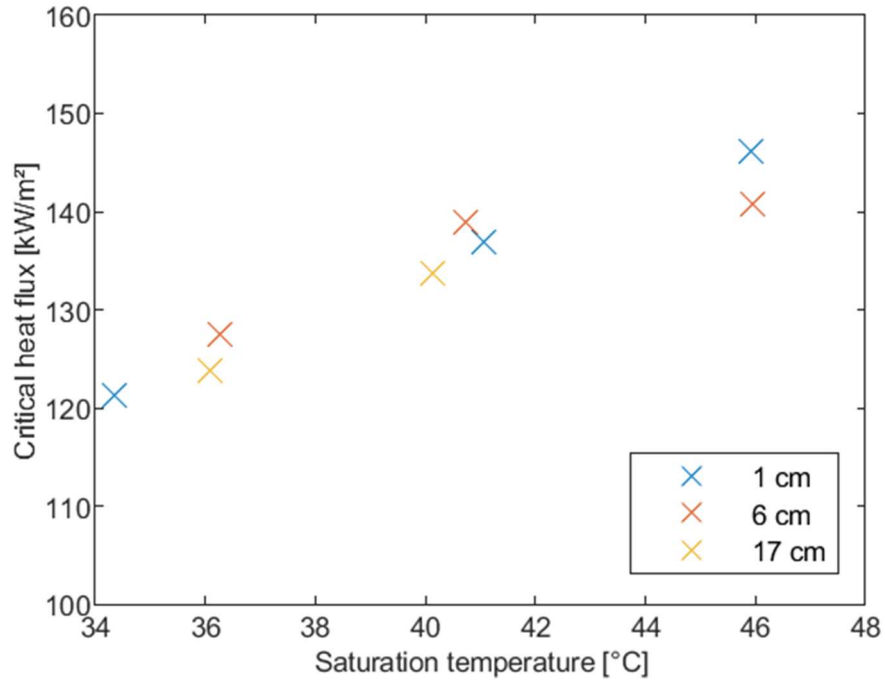


Fig. 8 Critical heat flux as a function of saturation temperature for varying liquid height

The measured CHF values are also compared to those predicted with correlations. The required fluid properties of FK-649 are determined using the REFPROP program [20], which determines the equation of state from McLinden et al. [21] and the surface tension from Cui et al. [22]. The predicted CHF is shown as a function of the measured CHF on figure Fig. 9 for both the Lienhard-Dhir and the Mudawar et al. correlations. The former predicts the CHF within 10% and the latter within 11%, making both a good option for assessing the maximal heat flux that can be transferred by pool boiling cooling. This indicates that the existing correlations for CHF can be applied for power module baseplate pool boiling cooling.

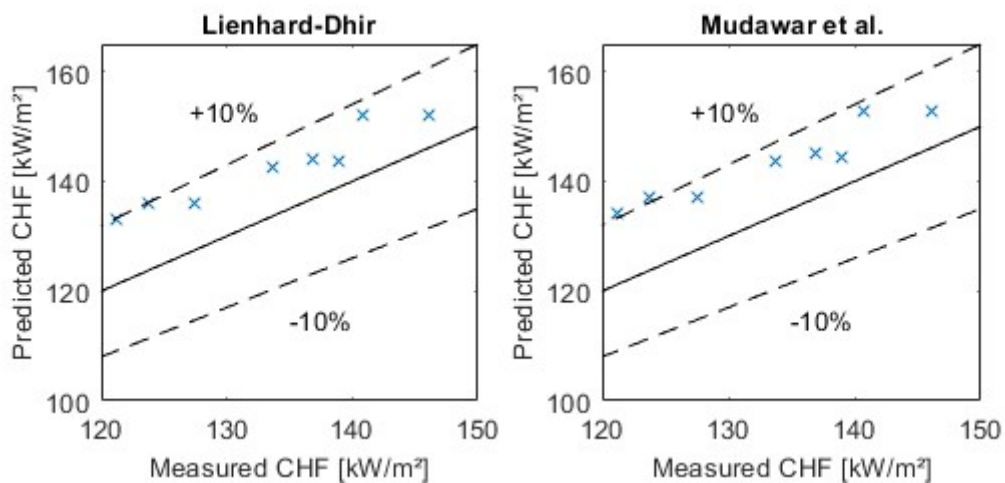


Fig. 9 Predicted CHF by the correlations as a function of the measured CHF for the Lienhard-Dhir correlation (left) and the Mudawar et al. correlation (right)

The largest CHF measured is equal to 146 kW/m², which is significantly lower than the maximal heat fluxes expected from the power module (around 300 kW/m²). It can be concluded that although the surface superheat temperatures for pool boiling on a flat baseplate are low for heat fluxes below the critical heat flux, the method is not sufficient for cooling power modules at the highest loads. Other strategies to increase the CHF should be investigated, such as using forced two-phase cooling and increasing the heat transfer area.

4. Conclusions

An experimental measurement campaign is done to determine the heat transfer and critical heat flux of pool boiling cooling of an inverter power module. FK-649, a low-GWP refrigerant is used as coolant.

Boiling curves were determined which are consistent with previous studies of other refrigerants. The boiling curve can be divided in three zones with different slopes: at low heat flux (close to onset of nucleate boiling), at intermediate heat flux and at high heat flux (close to the critical heat flux). The boiling curve is not affected by changes in liquid height from 1 cm to 17 cm. A higher saturation temperature leads to enhanced heat transfer.

Critical heat flux values up to 146 kW/m² were measured. The critical heat flux is not affected by changes in liquid height from 1 cm to 17 cm. For saturation temperatures ranging from 36 °C to 46 °C, the critical heat flux increases with saturation temperature. The measured critical heat flux is predicted within 10% by the correlation of Lienhard-Dhir.

Although high heat transfer coefficients are measured, heat fluxes at high loads of the power module exceed the critical heat flux. Further research should be concentrated on overcoming this obstacle, for example by applying flow boiling cooling or by increasing the heat transfer surface.

Conflict of interest

On behalf of all authors, the corresponding author states that there is no conflict of interest.

References

1. Emadi A, Lee YJ, Rajashekara K (2008) Power Electronics and Motor Drives in Electric, Hybrid Electric, and Plug-In Hybrid Electric Vehicles. *IEEE Trans Ind Electron* 55:2237–2245. <https://doi.org/10.1109/TIE.2008.922768>
2. Chu RC (2005) The Challenges of Electronic Cooling: Past, Current and Future. *J Electron Packag* 126:491–500. <https://doi.org/10.1115/1.1839594>
3. Pioro IL, Rohsenow W, Doerffer SS (2004) Nucleate pool-boiling heat transfer. II: assessment of prediction methods. *Int J Heat Mass Transf* 47:5045–5057. <https://doi.org/10.1016/j.ijheatmasstransfer.2004.06.020>
4. El-Genk MS, Bostanci H (2003) Saturation boiling of HFE-7100 from a copper surface, simulating a microelectronic chip. *Int J Heat Mass Transf* 46:1841–1854. [https://doi.org/10.1016/S0017-9310\(02\)00489-1](https://doi.org/10.1016/S0017-9310(02)00489-1)
5. Zuber N (1958) On the stability of boiling heat transfer. *Trans Am Soc Mech Engrs* 80:
6. Liang G, Mudawar I (2018) Pool boiling critical heat flux (CHF) – Part 2: Assessment of models and correlations. *Int J Heat Mass Transf* 117:1368–1383. <https://doi.org/10.1016/j.ijheatmasstransfer.2017.09.073>

7. Lienhard JH, Dhir VK (1973) Hydrodynamic Prediction of Peak Pool-boiling Heat Fluxes from Finite Bodies. *J Heat Transf* 95:152–158. <https://doi.org/10.1115/1.3450013>
8. Mudawar I, Howard AH, Gersey CO (1997) An analytical model for near-saturated pool boiling critical heat flux on vertical surfaces. *Int J Heat Mass Transf* 40:2327–2339. [https://doi.org/10.1016/S0017-9310\(96\)00298-0](https://doi.org/10.1016/S0017-9310(96)00298-0)
9. Moreno G (2011) Two-Phase Cooling Technology for Power Electronics with Novel Coolants. National Renewable Energy Laboratory (NREL)
10. Barnes CM, Tuma PE (2009) Immersion Cooling of Power Electronics in Segregated Hydrofluoroether Liquids. American Society of Mechanical Engineers Digital Collection, pp 719–725
11. Forrest E, Buongiorno J, McKrell T, Hu L-W (2009) Pool boiling performance of Novec™ 649 engineered fluid
12. Forrest EC, Hu L-W, Buongiorno J, McKrell TJ (2013) Pool Boiling Heat Transfer Performance of a Dielectric Fluid With Low Global Warming Potential. *Heat Transf Eng* 34:1262–1277. <https://doi.org/10.1080/01457632.2013.793103>
13. Gess JL, Bhavnani SH, Johnson RW (2015) Experimental Investigation of a Direct Liquid Immersion Cooled Prototype for High Performance Electronic Systems. *IEEE Trans Compon Packag Manuf Technol* 5:1451–1464. <https://doi.org/10.1109/TCPMT.2015.2453273>
14. Kaniowski R, Pastuszko R, Nowakowski Ł (2017) Effect of geometrical parameters of open microchannel surfaces on pool boiling heat transfer. *EPJ Web Conf* 143:02049. <https://doi.org/10.1051/epjconf/201714302049>
15. Bartle RS, Menon K, Walsh E (2018) Pool boiling of resin-impregnated motor windings geometry. *Appl Therm Eng* 130:854–864. <https://doi.org/10.1016/j.applthermaleng.2017.11.053>
16. Ghaffari O, Grenier F, Morissette J-F, Bolduc M, Jasmin S, Sylvestre J (2019) Pool Boiling Experiment of Dielectric Liquids and Numerical Study for Cooling a Microprocessor. In: 2019 18th IEEE Intersociety Conference on Thermal and Thermomechanical Phenomena in Electronic Systems (ITherm). pp 540–545
17. Cao Z, Wu Z, Sundén B (2019) Heat transfer prediction and critical heat flux mechanism for pool boiling of NOVEC-649 on microporous copper surfaces. *Int J Heat Mass Transf* 141:818–834. <https://doi.org/10.1016/j.ijheatmasstransfer.2019.07.036>
18. T’Jollyn I, Nonneman J, Hallemans L, Ravyts S, Driesen J, De Paepe M (2020) Experimental study of inverter base plate cooling with two-phase pool boiling. In: 33rd International Conference on Efficiency, Cost, Optimization, Simulation and Environmental Impact of Energy Systems (ECOS 2020). ECOS 2020 Organizing Committee, pp 83–91
19. Bell IH, Wronski J, Quoilin S, Lemort V (2014) Pure and Pseudo-pure Fluid Thermophysical Property Evaluation and the Open-Source Thermophysical Property Library CoolProp. *Ind Eng Chem Res* 53:2498–2508. <https://doi.org/10.1021/ie4033999>

20. Lemmon E, Bell IH, Huber M, McLinden M (2018) NIST Standard Reference Database 23: Reference Fluid Thermodynamic and Transport Properties-REFPROP, Version 10.0, National Institute of Standards and Technology. Stand Ref Data Program Gaithersburg
21. McLinden MO, Perkins RA, Lemmon EW, Fortin TJ (2015) Thermodynamic Properties of 1, 1, 1, 2, 2, 4, 5, 5, 5-Nonafluoro-4-(trifluoromethyl)-3-pentanone: Vapor pressure,(p, ρ , T) Behavior, and Speed of Sound Measurements, and an Equation of State. *J Chem Eng Data* 60:3646–3659
22. Cui J, Yan S, Bi S, Wu J (2018) Saturated Liquid Dynamic Viscosity and Surface Tension of trans-1-Chloro-3,3,3-trifluoropropene and Dodecafluoro-2-methylpentan-3-one. *J Chem Eng Data* 63:751–756. <https://doi.org/10.1021/acs.jced.7b00902>

Statements and Declarations

The authors declare that no funds, grants, or other support were received during the preparation of this manuscript. The authors have no relevant financial or non-financial interests to disclose.